

Comparing Numerical Integration Schemes for Time-Continuous Car-Following Models

Martin Treiber^{a,*}, and Venkatesan Kanagaraj^b

^a*Technische Universität Dresden, Institute for Transport & Economics,
Würzburger Str. 35, D-01187 Dresden, Germany*

^b*TechnionIsrael Institute of Technology, Haifa 32000, Israel.*

Abstract

When simulating trajectories by integrating time-continuous car-following models, standard integration schemes such as the forth-order Runge-Kutta method (RK4) are rarely used while the simple Euler's method is popular among researchers. We compare four explicit methods: Euler's method, ballistic update, Heun's method (trapezoidal rule), and the standard forth-order RK4. As performance metrics, we plot the global discretization error as a function of the numerical complexity. We tested the methods on several time-continuous car-following models in several multi-vehicle simulation scenarios with and without discontinuities such as stops or a discontinuous behavior of an external leader. We find that the theoretical advantage of RK4 (consistency order 4) only plays a role if both the acceleration function of the model and the external data of the simulation scenario are sufficiently often differentiable. Otherwise, we obtain lower (and often fractional) consistency orders. Although, to our knowledge, Heun's method has never been used for integrating car-following models, it turns out to be the best scheme for many practical situations. The ballistic update always prevails Euler's method although both are of first order.

Key words: time-continuous car-following model; numerical integration; Euler's method; ballistic update; trapezoidal rule; Heun's method; Runge-Kutta method; consistency order

* Corresponding author. Tel.: +49 351 463 36794; fax: +49 351 463 36809
Email address: treiber@vwi.tu-dresden.de (Martin Treiber).
URL: <http://www.mtreiber.de> (Martin Treiber).

1 Introduction

Time-continuous car-following models (or more precisely, their longitudinal dynamics components) prescribe the acceleration of individual cars as a function of the driver’s characteristic behaviour and the surrounding traffic. Formally, their mathematical formulation is equivalent to that of physical particles following Newtonian dynamics with the physical forces replaced by “social forces” (Helbing and Tilch, 1998). In contrast to car-following models formulated in discrete time (coupled maps) or fully discretely (cellular automata), time-continuous car-following models must be augmented with a numerical integration method in all but the most trivial analytically solvable cases (Treiber and Kesting, 2013).

Mathematically speaking, time-continuous car-following models without explicit reaction time delay represent coupled ordinary differential equations (ODE). The most popular models of this class are the optimal-velocity model (OVM) of Bando et al. (1994), derivatives such as the full-velocity difference model (FVDM) of Jiang et al. (2001), and the Intelligent-Driver Model (IDM) by Treiber et al. (2000). Early car-following models such as that by Gazis, Herman and Rothery (GHR, Gazis et al. (1961)) or the linear ACC model by Helly (1959) also fall into this class.

Because of the complexity and possible event-oriented components of traffic flow scenarios, one generally assumes a fixed common time step h and explicit numerical schemes to obtain trajectories from the model equations. In the general literature on numerical mathematics (see, e.g., Quarteroni et al. (2007)), the standard explicit numerical integration scheme for ODEs is the fourth-order Runge-Kutta method (RK4). However, in the domain of microscopic traffic flow modelling, the use of this method is rarely stated (counterexamples include Kaupuzs et al. (2004) and Shamoto et al. (2011)). Instead, most authors apply simpler methods or do not specify the numerical method at all. Commonly used schemes are the simple Euler method (Aw et al., 2002) or the ballistic update assuming constant accelerations during one time step (Treiber and Kesting, 2013). Notice that also the open-source traffic simulators SUMO (Behrisch et al., 2011) and AIMSUN (Casas et al., 2010) use simple Euler update for the positions.

Sometimes, time-continuous models plus a lower-order update method are proposed as time-discrete models in their own right. For example, Newell’s microscopic model (Newell, 1961) corresponds to an OVM with a triangular fundamental diagram and simple Euler-update with a time step h equal to the desired time gap (Treiber and Kesting, 2013). Similarly, a time-discrete model has been derived from the GHR model by using Euler update with h equal to the reaction time, and qualitatively different behavior

has been found compared to integrating the original GHR model with the RK4 method (Jamison and McCartney, 2009). In the context of car-following methods, the ballistic method is particularly appealing since it allows to model reaction times without introducing explicit delays which would transform the ODEs of time-continuous car-following models (such as all time-continuous models mentioned above) into delay-differential equations. It has been shown (Kesting and Treiber, 2008) that integration of the IDM by the ballistic method with time step h is essentially equivalent to an explicit reaction time delay $T_r = h/2$ of the corresponding delay-differential equations (which are, then, integrated by higher-order methods or very small time steps).

Nevertheless, it is often desired to approach the true solution of time-continuous car-following models as closely as possible. A criterion for the quality of an integration scheme is its (local or global) consistency order stating how fast the approximate numerical solution converges to the true solution when decreasing the time step h (Quarteroni et al. (2007), see Sect. 2 for details). However, for practical integration steps h , higher-order methods do not necessarily lead to lower discretization errors. Moreover, if the acceleration function of the model is not sufficiently smooth (differentiable) or the simulation scenario contains discontinuities such as stops, lane changes, or traffic lights, the actual consistency order of a given numerical scheme is generally lower than its nominal order (Quarteroni et al., 2007). Finally, higher-order methods need several evaluations of the model’s acceleration function per vehicle and per time step while Euler’s method and the ballistic scheme need only one.

This leads to following question: “Does the higher numerical accuracy of higher-order schemes outweigh their higher numerical complexity in terms of computation time, for practical cases?” Specifically, we would like to know which numerical scheme has the lowest global discretization error for a given numerical complexity, and how this depends on the model and the simulation scenario.

In this work, we profile four numerical methods, simple Euler, ballistic scheme, Heun’s rule or trapezoidal rule, and RK4, for three car-following models (OVM, FVDM, IDM) in several multi-vehicle simulation scenarios. We found that RK4 is, in fact, superior if certain rather restrictive conditions for the differentiability of the acceleration function and the external data are satisfied, and if a high numerical precision is required. In most practical situations, however, the ballistic scheme and the trapezoidal rule turn out to be the most efficient and robust methods, although the latter is rarely used. Moreover, the ballistic update always prevails simple Euler although both are of first order.

In the next section, we specify the integration schemes in the context of car-following models. In Sect. 3, we describe the simulation tests, define the nu-

merical complexity as a measure for the computational burden, and the discretization error in terms of a vector norm on the deviations of the trajectories. In Sect. 4, we present the simulations and results. Finally, Sect. 5 gives a discussion and an outlook.

2 Integration Schemes for Car-Following Models and their mathematical properties

2.1 Mathematical Formulation

We start by writing the dynamics created by a time-continuous car-following models without explicit reaction time as a general system of ordinary differential equations,

$$\frac{d\vec{y}}{dt} = \vec{f}(\vec{y}, t). \quad (1)$$

The state vector \vec{y} represents all positions and speeds, and $\vec{f}(\cdot)$ characterizes the specific car-following model and possibly external data such as an externally driven leading vehicle. Specifically, we consider a class of car-following models defined by

$$\frac{dx_i}{dt} = v_i, \quad (2)$$

$$\frac{dv_i}{dt} = a^{\text{mic}}(s_i, v_i, v_{i-1}), \quad (3)$$

where $i = 1, \dots, n$ denotes the index of a fixed number n of vehicles (the first vehicle has the lowest index), x_i denotes the position of the front bumper of vehicle i , v_i its speed, and $s_i = x_{i-1} - x_i - l_{i-1}$ the bumper-to-bumper gap where l_{i-1} is the length of the leading vehicle.

A model of this class is specified by the acceleration function $a^{\text{mic}}(s, v, v_l)$. The simulation scenario is specified by the number n of vehicles following each other, by the initial conditions $x_i(0)$ and $v_i(0)$ for all vehicles i , and by a boundary condition prescribing the acceleration $a_1(v_1, t)$ of the first vehicle $i = 1$. Specifically, we consider free-flow boundary conditions (Treiber and Kesting, 2013),

$$a_1(v_1, t) = a_{\text{free}}(v_1) = a^{\text{mic}}(\infty, v_1, v_1), \quad (4)$$

and externally prescribed leader acceleration profiles

$$a_1(v_1, t) = a_{\text{ext}}(t). \quad (5)$$

Periodic boundary conditions,

$$a_1(v_1, v_n, x_1, x_n) = a^{\text{mic}}(x_n + L_{\text{road}} - x_1 - l_n, v_1, v_n) \quad (6)$$

would be possible as well, as would be external influences such as traffic lights. However, we do not allow open boundary conditions (sources and/or sinks) since the ensuing time dependent vehicle number n would violate the general form (1). Nevertheless, we do not expect that open boundary conditions will influence our results in any significant way.

In order to cast the model equations (2) and (3) into the general form (1), we define the state vector as

$$\vec{y} = \begin{pmatrix} \vec{x} \\ \vec{v} \end{pmatrix} = (x_1, \dots, x_n, v_1, \dots, v_n)^T. \quad (7)$$

Then, the right-hand side of (1) becomes

$$\vec{f}(\vec{y}, t) = \begin{pmatrix} \vec{v} \\ \vec{a}(\vec{x}, \vec{v}, t) \end{pmatrix} = \begin{pmatrix} v_1 \\ \vdots \\ v_n \\ a_1(v_1, t) \\ a^{\text{mic}}(x_1 - x_2 - l_1, v_2, v_1) \\ \vdots \\ a^{\text{mic}}(x_{n-1} - x_n - l_{n-1}, v_n, v_{n-1}) \end{pmatrix}. \quad (8)$$

Notice that the external boundary condition (5) makes the right-hand side non-autonomous (the independent variable t appears explicitly) while, for free or periodic boundary conditions, the ODE is autonomous.

2.2 Convergence and consistency order

The quality of explicit numerical integration method with respect to discretization errors is generally characterized by its consistency order p . A method has a *local* consistency order $p_{\text{loc}} > 0$ within a region R of state variables \vec{y} and times t if it converges to the true solution $\vec{y}(t)$ and if, for all integration time steps $h > 0$ and all $\{\vec{y}, t\} \in R$, the inequality

$$\epsilon_{\text{loc}} \equiv \frac{\| \vec{y}_{\text{num}}(t+h) - \vec{y}(t+h) \|}{h} < Ah^{-p_{\text{loc}}} \quad (9)$$

is satisfied. Here, ϵ_{loc} is the local truncation error, $\vec{y}_{\text{num}}(t+h)$ is the numerical approximation for the true initial condition $\vec{y}(t)$, $\| \cdot \|$ is some vector norm (see Sect. 3.3), A is a positive prefactor, and the consistency order is the highest positive value of p_{loc} for which this inequality is satisfied. The denominator h ensures that the decreasing numerical errors are not a trivial consequence of decreasing time steps h .

More relevant for simulations of car-following models, however, is the *global* consistency order indicating how the cumulated discretization errors of a complete simulation run decrease with decreasing h . If the simulation starts at $t = 0$ with given initial conditions $\vec{y}(0) = \vec{y}_0$ and ends at $t = T$, one may define the global consistency order by the highest value of p_{glob} for which

$$\epsilon_{\text{glob}} \equiv \| \vec{y}_{\text{num}} - \vec{y} \| < Ah^{-p_{\text{glob}}} \quad (10)$$

is satisfied for a finite prefactor A and all $h > 0$. Here, $\| \cdot \|$ is a vector norm on all the components of \vec{y} for all time steps, see (18) or (19) below.

If the right-hand side $\vec{f}(\vec{y}, t)$ is Lipschitz continuous in the whole region R covered by the trajectories, one can show (Quarteroni et al., 2007) that (i) the true solution exists, (ii) it is unique, and (iii) converging numerical methods have a unique consistency order $p_{\text{loc}} = p_{\text{glob}} = p$. The function $\vec{f}(\vec{y}, t)$ is Lipschitz continuous if it is differentiable with respect to the components of \vec{y} nearly everywhere and if the gradients are bounded. We notice that, for car-following models, these are nontrivial requirements. For example, they are not satisfied for any car-following model with a discontinuous acceleration function. In contrast, a non-differentiability at certain points, typically introduced by min- or max conditions, is allowed. Even for a perfectly smooth acceleration function as that of the IDM, the Lipschitz condition is violated for gaps $s \rightarrow 0$ (crashes) or diverging speeds or speed differences. While the latter can be excluded by the general dynamics of the trajectories, the former can only be verified a posteriori. In the following, we will base our investigations on the global discretization error (truncation error) ϵ_{glob} as defined in (10).

Finally, we note that the prefactor A indicating the upper bound varies wildly with the method and the problem at hand. Generally, A increases drastically with the order of the method, if the situation includes abrupt changes of the state, e.g., stop-and-go traffic. These variations are of a high practical relevance since they imply that a higher consistency order not necessarily leads to a higher accuracy as we will show in Sect. 4.

2.3 The investigated integration methods

We investigate (i) the simple Euler's method, (ii) the trapezoidal rule (Heun's method), (iii) the standard fourth-order Runge-Kutta method (RK4), and (iv) the ballistic update. For reference, the methods (i) - (iii) for integrating (1) are as follows:

$$\begin{aligned} \text{Euler:} \quad \vec{k}_1 &= \vec{f}(\vec{y}, t), \\ \vec{y}(t+h) &= \vec{y} + h\vec{k}_1, \end{aligned} \tag{11}$$

$$\begin{aligned} \text{trapezoidal:} \quad \vec{k}_1 &= \vec{f}(\vec{y}, t), \quad \vec{k}_2 = \vec{f}(\vec{y} + h\vec{k}_1, t+h), \\ \vec{y}(t+h) &= \vec{y} + \frac{h}{2}(\vec{k}_1 + \vec{k}_2), \end{aligned} \tag{12}$$

$$\begin{aligned} \text{RK4:} \quad \vec{k}_1 &= \vec{f}(\vec{y}, t), \quad \vec{k}_2 = \vec{f}\left(\vec{y} + \frac{h}{2}\vec{k}_1, t + \frac{h}{2}\right), \\ \vec{k}_3 &= \vec{f}\left(\vec{y} + \frac{h}{2}\vec{k}_2, t + \frac{h}{2}\right), \quad \vec{k}_4 = \vec{f}(\vec{y} + h\vec{k}_3, t+h), \\ \vec{y}(t+h) &= \vec{y} + \frac{h}{6}(\vec{k}_1 + 2\vec{k}_2 + 2\vec{k}_3 + \vec{k}_4). \end{aligned} \tag{13}$$

The ballistic method is only defined for the special case that the ODE (1) represents dynamic acceleration equations for one or several particles which, of course, includes time-continuous car-following models. The ballistic method assumes constant accelerations during one time step which will be taken as that at the beginning of this step:

$$\vec{y}(t+h) = \begin{pmatrix} \vec{x}(t+h) \\ \vec{v}(t+h) \end{pmatrix} = \begin{pmatrix} \vec{x} \\ \vec{v} \end{pmatrix} + h \begin{pmatrix} \vec{v} \\ \vec{a}(\vec{x}, \vec{v}) \end{pmatrix} + \frac{1}{2}h^2 \begin{pmatrix} \vec{a}(\vec{x}, \vec{v}) \\ \vec{0} \end{pmatrix}. \tag{14}$$

This can be interpreted as a mixed first-order, second-order update consisting of an Euler update for the speeds, and a trapezoidal update for the positions. While the resulting order $p = 1$ is that of Euler's method, it turns out that the prefactor A is significantly lower in nearly all situations. As for the Euler update, the acceleration function $\vec{a}(\vec{x}, \vec{v})$ needs only to be calculated once per update step while two and four calculations are necessary for the trapezoidal and RK4 updates, respectively. Since calculating the acceleration function represents the essential part of the numerical complexity, this gives a hint at the numerical efficiency of the ballistic update.

2.4 Special Treatment for Stopping Vehicles

To be fully effective, the general numerical methods assume smoothness conditions on the model and the data that are rarely given when simulating car-following models. Regarding a common source of such discontinuities, vehicle stopping, we can nevertheless improve all methods in a systematic way by overriding the canonical formulation for such a situation. Due to the finite update times, all update formulas (11) - (14) will lead to negative speeds whenever a time step includes the stopping of vehicles. In this case, it would be better to estimate the stopping position directly. Specifically, we have applied, for all methods, following heuristics:

- The special treatment is activated if, for a vehicle i , the speed of a predictor or the final step of an integration scheme is negative indicating that this vehicle has stopped at some time instant of this time step. It also implies that the acceleration $a_i^{\text{mic}}(t)$ calculated at the begin of this time step is negative.
- In case of activation, we override the originally calculated position by the ballistic heuristics

$$x_i(t + \tilde{h}) = x_i(t) - \frac{v_i^2(t)}{2a_i^{\text{mic}}(t)} \quad \text{if} \quad v_i(t) + \tilde{h}a_i^{\text{mic}}(t) < 0. \quad (15)$$

Here, \tilde{h} is either h or $h/2$ (for the second and third predictor of RK4).

- Additionally, in case of activation, we reset the speed to zero.

This provision for stopping vehicles fits naturally to the ballistic approach but improves the other methods as well. For the higher-order methods, it increases the maximum effective consistency order from $p = 1$ to 2 and decreases the absolute error, at least, if stopped vehicles are the only reason for non-smooth trajectories.

3 Methodology for Assessing the Integration Schemes

In order to assess the numerical schemes, we need to specify the numerical complexity, the global discretization error, and the reference solution against which to calculate the global error. Since the true solution cannot be obtained for any nontrivial scenario (otherwise, there would be no need for simulation), setting up the reference (or, more precisely, an estimator for the reference with controlled errors), is a nontrivial task.

3.1 Numerical complexity

We define numerical complexity as the computation time to simulate a single vehicle on a single lane over a given simulated time interval, e.g., 1 s. The inverse of this quantity indicates the number of vehicles that can be simulated in real time. Since nearly all of the computational burden consists in evaluating the model’s acceleration function and a model of nominal consistency order p needs p calculations per time step, the numerical complexity is essentially proportional to the quantity

$$C = \frac{p}{h} \quad (16)$$

denoting the number of evaluations of the acceleration function per vehicle and simulated unit time. The nominal consistency order is $p = 1$ for the Euler and ballistic updates, $p = 2$ for the trapezoidal rule, and $p = 4$ for RK4.

3.2 Reference Solution

While a unique exact global solution exists for our simulation scenarios (cf. Sec. 2.2), it cannot be calculated analytically for any but the most trivial situations. We therefore calculate a “reference solution” $\vec{y}_{\text{ref}}(t)$ against which to compare the integration schemes by the RK4 scheme using a time step $h_{\text{ref}} = 10^{-4}$ s which is smaller than the smallest time step of the actual investigations by a factor of 200. To test the validity of this reference, we repeat the calculation with $h = 2h_{\text{ref}}$ resulting in $\vec{y}_{\text{cmp}}(t)$ and calculate the global error between these two solutions. Assuming that the *actual* global consistency order of RK4 for a given scenario is $p_{\text{act}} \geq 1$ (which can only be confirmed *a posteriori*) this provides an upper bound for the global error between the reference and the unknown true solution (Quarteroni et al., 2007):

$$\| \vec{y}_{\text{ref}} - \vec{y} \| \leq \| \vec{y}_{\text{cmp}} - \vec{y}_{\text{ref}} \| \quad (17)$$

This controlled error of the reference solution ensures that all global discretization errors calculated in the following can be determined with uncertainties (i.e., second-order errors) of less than 1 %.

3.3 Global Discretization Error

We have tested several global error norms, among them the 1-norms and 2-norms of the time series of location, speed, acceleration, and gap for one or more trajectories, and combinations thereof. Examples include the 1-norm of

the speed trajectory of the i^{th} follower,

$$\epsilon_i = \|v_i^{\text{num}} - v_i^{\text{ref}}\| = \frac{1}{m} \sum_{j=1}^m |v_i^{\text{num}}(jh) - v_i^{\text{ref}}(jh)|, \quad (18)$$

where $v_i^{\text{num}}(jh)$ is the speed of the i^{th} vehicle at time $t = jh$ (after the j^{th} time step), and $v_i^{\text{ref}}(jh)$ is the corresponding speed of the reference solution.

Another example is the 1-norm of the speeds of all trajectories,

$$\epsilon = \|\vec{v}^{\text{num}} - \vec{v}\| = \frac{1}{nm} \sum_{i=1}^n \sum_{j=1}^m |v_i^{\text{num}}(jh) - v_i^{\text{ref}}(jh)|, \quad (19)$$

where $\vec{v}(t) = (v_1(t), \dots, v_n(t))^T$.

Since we always obtained similar results, regardless of the quantity (speed or gap) or the chosen vehicle trajectory (or including all trajectories), we will, henceforth, only consider ϵ_{10} , i.e., the discretization errors of the speeds of the 10th vehicle.

4 Results

As main test cases for the simulations, we have used the city start-stop scenario as described in Chapter 11 of Treiber and Kesting (2013): Initially, a queue of 20 identically parameterized cars is waiting behind a red traffic light. At $t = 0$, the traffic light turns green and the queue of cars starts moving until a red traffic light 670 m ahead stops the vehicle platoon again. Most tests are performed with the IDM or variants thereof parameterized according to either the second or the third column of Table 1.

In the theoretical “best case”, both the acceleration function of the model and, if applicable, external data (such as externally prescribed leading trajectories) are smooth, i.e., infinitely often differentiable. This will produce smooth trajectories for which all mathematical conditions for the theoretical consistency order are satisfied. We will start with this ideal case before we simulate less ideal (and more realistic) scenarios by progressively reducing the degree of smoothness.

4.1 Smooth Trajectories

Figure 1 shows some of the resulting trajectories when parameterizing the IDM according to the second column of Table 1. When restricting the simula-

Parameter	Standard set	“creep-to-stop” set
desired speed v_0	15 m/s	15 m/s
time gap parameter T	1 s	1 s
minimum gap s_0	2 m	1 m
maximum acceleration a	1 m/s ²	2 m/s ²
comfortable deceleration b	1.5 m/s ²	1.5 m/s ²

Table 1
IDM parameters of the tests.

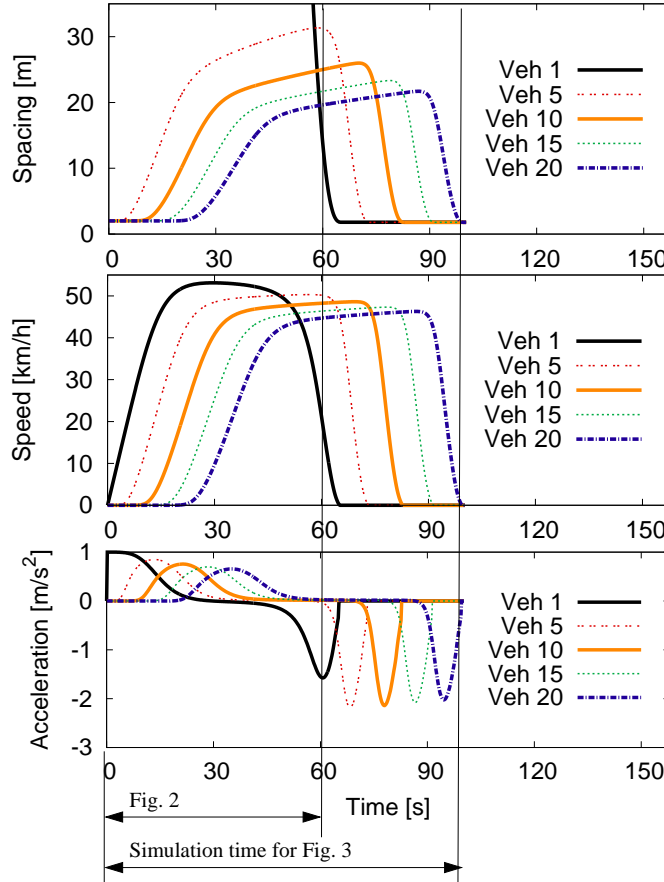


Fig. 1. Trajectories of the start-stop scenario: single-lane city traffic between two signalized intersections as simulated with the IDM with standard parameters.

tion time to 60 s, no vehicle has stopped yet at the end of the simulation time. Since, for nonzero speeds, the IDM acceleration function and the resulting trajectories are smooth, this means that the conditions for the maximum theoretical consistency orders are satisfied, i.e., $p = 1$ for Euler’s and the ballistic methods, $p = 2$ for the trapezoidal rule, and $p = 4$ for RK4 method.

Figure 2 shows the numerical accuracy of the 60 s-simulation in form of a log-log plot of the discretization errors as a function of the numerical costs for all

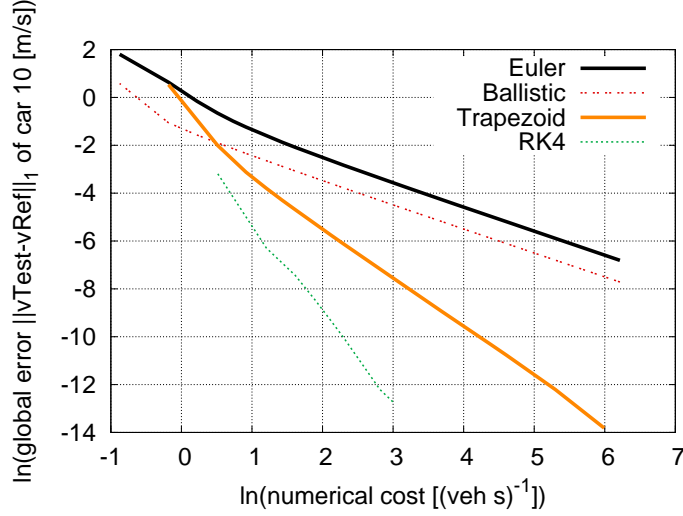


Fig. 2. Error norm of the speeds as a function of the numerical complexity for four numerical integration methods. The simulation is that of Fig. 1 for the simulation interval $[0 \text{ s}, 60 \text{ s}]$.

four integration methods presented in Sec. 2. As error measure, we used the 1-norm ϵ_{10} of the speed differences of the 10th follower. Specifically, we have assumed 16 different update times ranging from $h = 0.002 \text{ s}$ to $h = 2.4 \text{ s}$. The reference trajectory was obtained by applying the RK4 method with an update time step $h = 10^{-4} \text{ s}$. We recorded the result every 2.4 s which is the lowest common multiple of all update intervals h used for the test simulations. This is necessary to separate the discretization errors to be analyzed from errors when interpolating data points and provides a common data basis for all test simulations. As measure for the numerical cost C , we defined the number of calculations of the acceleration function per simulated vehicle and simulated second according to Eq. (16).

We observe that the theoretical consistency orders are realized in the actual simulation, i.e., the asymptotic negative slopes p_{sim} of the log-log plot are approximatively equal to $p = 1$ for the Euler and ballistic schemes, $p = 2$ for the trapezoidal scheme, and $p = 4$ for RK4. Moreover, for $h \leq 0.5 \text{ s}$ (which corresponds to $C \geq 2p$ and includes the practically used intervals), the order of performance of the methods (from best to worst) is RK4, trapezoidal, ballistic, and Euler. Notice that the ballistic scheme is always superior to Euler's scheme (only about 30% of the error of the latter) although both have the same consistency order $p = 1$.

4.2 Discontinuous Accelerations Caused by Stopped Vehicles

We simulate the same city start-stop scenario as above with the same parameter set, but now for a simulation time of $t_{\text{max}} = 100 \text{ s}$ instead of 60 s . As shown

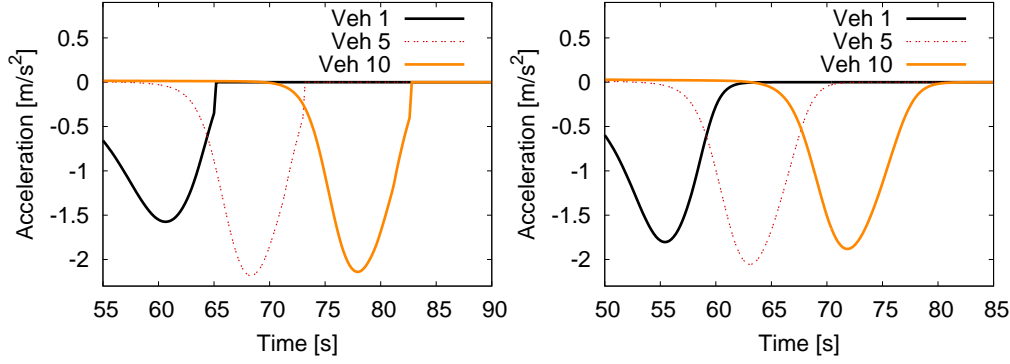


Fig. 3. Detail of the acceleration profile during the stopping phase. Left: distinct stop (parameterization by the second column of Table 1); right: creeping stop (third column)

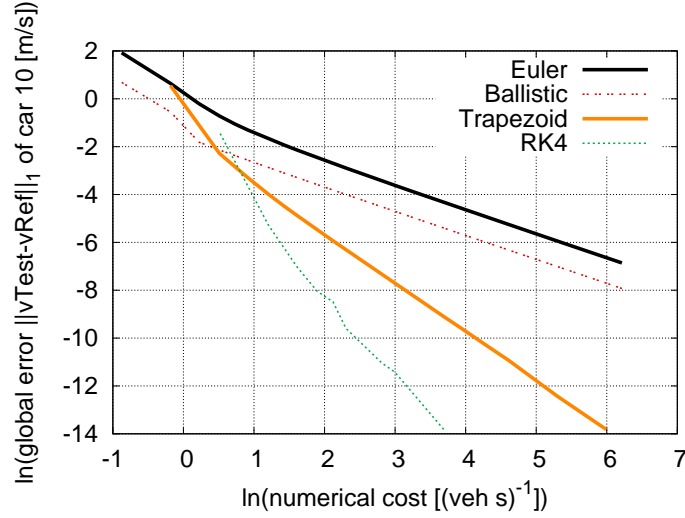


Fig. 4. As Fig. 2 but for a total simulation interval of 100 s.

in Fig. 3, some vehicles have stopped with a discontinuous acceleration profile after this prolonged time. For the higher-order methods, this means that the mathematical smoothness conditions for the theoretical consistency order are no longer satisfied.

Does this have implications for the actual accuracy? Figure 4 shows that the consistency orders of the Euler, ballistic, and trapezoidal schemes essentially retain their theoretical values of $p = 1$, 1 , and 2 , respectively. Furthermore, the prefactors A of Eq. (10) determining the absolute size of the discretization errors are essentially unchanged as well. In contrast, the errors of the RK4 method significantly increase by a factor of about five. Nevertheless, RK4 remains the best method for practical update intervals. Remarkably, its simulated consistency order $p \approx 3.5$ is only marginally below its theoretical value of 4 . At first sight, this is unexpected since, for mathematical reasons, the consistency order for a discontinuous acceleration profile should not exceed

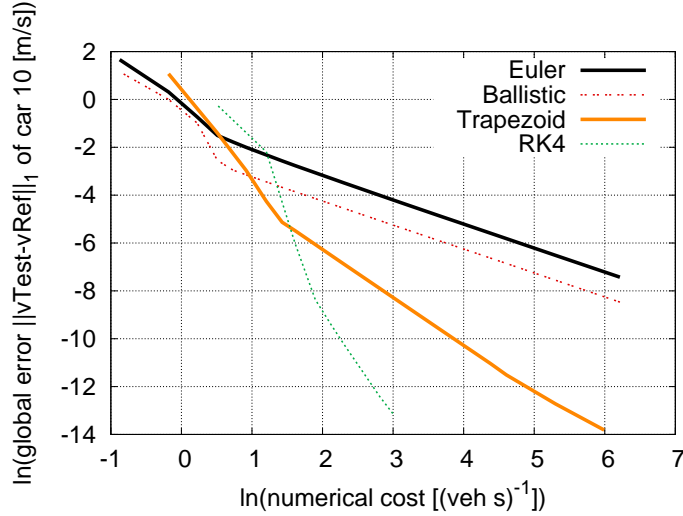


Fig. 5. Discretization errors of the scenario of Fig. 4 when re-parameterizing the IDM by the 3rd column of Table 1 resulting in a creeping halt.

$p = 1$, regardless of the method.

There are two reasons to explain these findings. Firstly, the discontinuity concerns just a single point, so the error contribution of lower consistency order is small and the *asymptotic* slope may not yet have been reached in the log-log plots. Secondly, we have taken special provisions to increase the accuracy of the stopping situation: Whenever a predictor or the final value of an integration step yields a negative speed, we override the normal algorithm by setting the speed to zero and the position to the ballistically estimated stopping position which is calculated assuming a constant deceleration defined by the right-hand side of (8) for this step. This special-purpose procedure, which is described in Sec. 2.4 below in more detail, increases the upper bound of the expected consistency order to 2 in all simulations that include stops but have smooth acceleration functions and data, otherwise.

Depending on the parameterization, it is possible that the simulated vehicles do not stop at a precisely defined time (as above) but “creep to a halt” retaining a smooth acceleration profile at all times. An example parameterization for this behaviour is given by the third column of Table 1 resulting in the trajectories of Fig. 3 right. Then, the mathematical conditions for the full theoretical consistency order are satisfied again. In fact, the log-log plot of the discretization error vs. numerical cost (Fig. 5) shows little changes with respect to the first simulation without stops. Particularly, the slopes are consistent with the theoretical expectation again. However, the RK4 method produced significantly larger errors compared to the 60 s simulation when simulating with comparatively large update time intervals. We also simulated this scenario with the OVM of Bando et al. (1994) with typical parameters resulting in a creeping halt as well. Again, we found the expected theoretical consistency

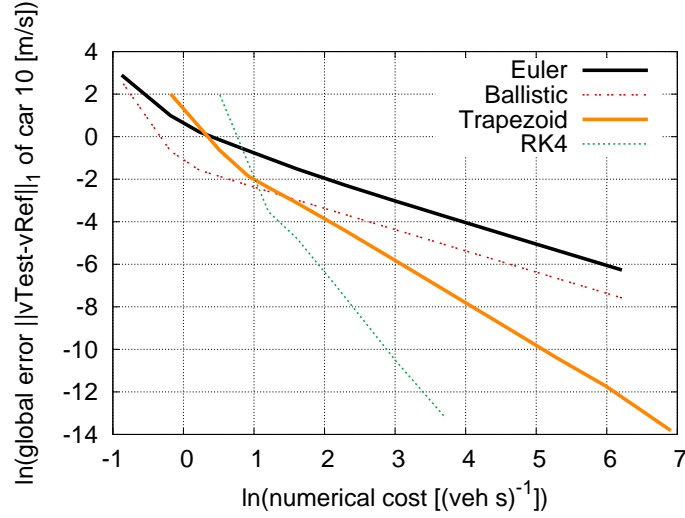


Fig. 6. Discretization errors when simulating the scenario of Fig. 4 with the optimal-velocity model (creeping halt).

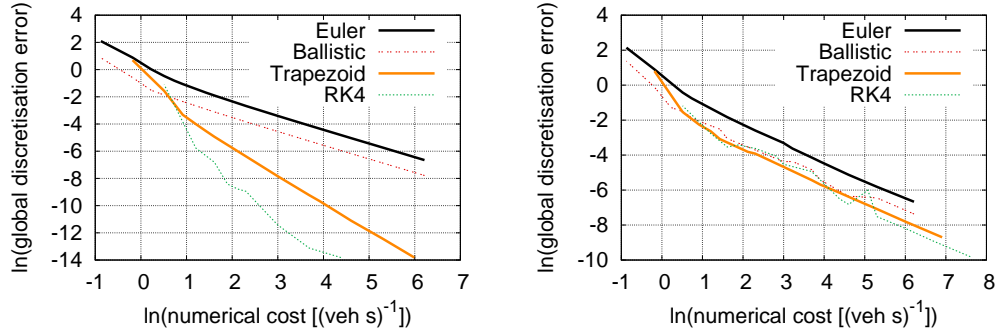


Fig. 7. Discretization errors of the start-stop scenario ($t_{\max} = 100$ s) for the IDM-Plus (left) and the modified IDM according to (23) (right). All IDM variants are parameterized according to the second column of Table 1.

orders but a higher prefactor, i.e., generally higher errors for all methods and all discretization time steps.

4.3 Non-Smooth Acceleration Functions

Discontinuous acceleration profiles do not only result when vehicles stop but may also be generated by the model itself if its acceleration function $a_{\text{mic}}(s, v, v_l)$ has regions in state space with kinks (non-differentiable points) or discontinuities, at least when the dynamics reaches these regions. We tested both cases by simulating the standard start-stop scenario ($t_{\max} = 100$ s) with two modifications of the IDM. As an example for an acceleration function with kinks, we simulated the “IDM-Plus” proposed by Schakel et al. (2012). Its acceleration function reads

$$a_{\text{IDM+}}^{\text{mic}}(s, v, v_l) = \min \left\{ a_{\text{free}}(v), a \left[1 - \left(\frac{s^*(v, v_l)}{s} \right)^2 \right] \right\} \quad (20)$$

with the usual IDM expressions for the free acceleration and the dynamic desired gap,

$$a_{\text{free}}(v) = a \left[1 - \left(\frac{v}{v_0} \right)^4 \right], \quad s^*(v, v_l) = \max \left[s_0 + vT + \frac{v(v - v_l)}{2\sqrt{ab}}, 0 \right]. \quad (21)$$

For reference, the acceleration function of the original IDM reads

$$a_{\text{IDM}}^{\text{mic}}(s, v, v_l) = a_{\text{free}}(v) - a \left(\frac{s^*(v, v_l)}{s} \right)^2. \quad (22)$$

The additional “min” condition of the IDM-Plus¹ leads to a kink in the acceleration profile when the remaining distance of the first vehicle to the red traffic light (modelled as a standing virtual vehicle of length zero) is approximatively $s_c = s_0 + v_0T + 1/2v_0^2/\sqrt{ab}$, and also to (smaller) kinks of the accelerations of the following vehicles.

Figure 7 (left) shows the discretization errors for the IDM-Plus. We observe that both the error prefactors and the consistency orders of the Euler, ballistic, and trapezoidal methods remains essentially unchanged while the consistency order of RK4 reduces to about two. This is expected on theoretical grounds: A kink in the realized acceleration profile sets the upper limit of the consistency order of any explicit method to $p_{\text{max}} = 2$. For practical simulation time intervals corresponding to a numerical cost of around $10 (\text{veh s})^{-1}$, however, we observe little difference with respect to discretization errors for a smooth acceleration profile.

To obtain a model with *discontinuities* in the acceleration function, we modified the free-flow IDM acceleration function to

$$a_{\text{free}}(v) = \begin{cases} a & v < v_0 \\ 1 - v/v_0 & v \geq v_0 \end{cases}. \quad (23)$$

In this model, drivers reduce their acceleration abruptly from a to zero once reaching their desired speed.

Figure 7 (right) shows that acceleration discontinuities greatly increase the discretization errors of the higher-order methods. In line with theoretical expectations, all methods now have the consistency order $p = 1$. Regarding the

¹ The “min” function of the dynamic desired gap of all IDM variants becomes only relevant in rare cases.

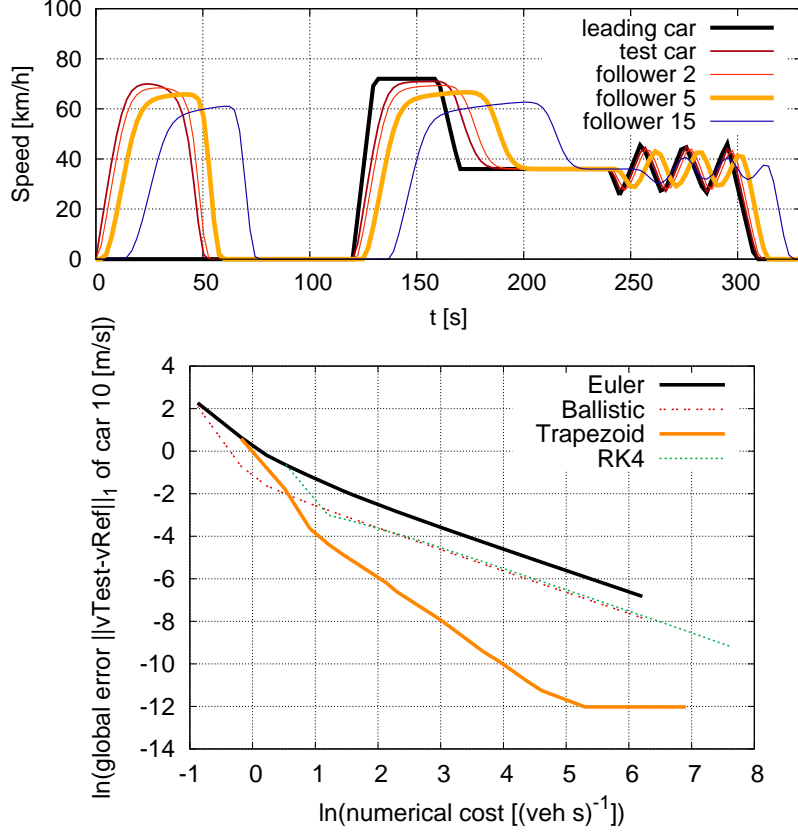


Fig. 8. Top: following a leader with a fixed speed profile (IDM, parameters as in the second column of Table 1); bottom: convergence diagram for the tenth follower.

absolute errors, Euler is worst while all other methods are essentially equivalent.

4.4 External Data with Discontinuous Accelerations

Another source of discontinuities can be external system data, e.g., prescribed speed profiles of an external leader. Figure 8 shows a simulation where a platoon of vehicles follows a leader with an externally given discontinuous acceleration profile corresponding to a speed profile with kinks. Assuming a model with a continuous acceleration function, this leads to an acceleration profile with kinks for the first follower, and to differentiable profiles for the further followers.

The log-log plot of the discretization errors (Fig. 8 bottom) reveals that the Euler, ballistic, and trapezoidal methods have their expected consistency orders and absolute errors while, surprisingly, RK4 has only consistency order $p = 1$. It seems that, at each abrupt behavioral change of the leader, the pre-

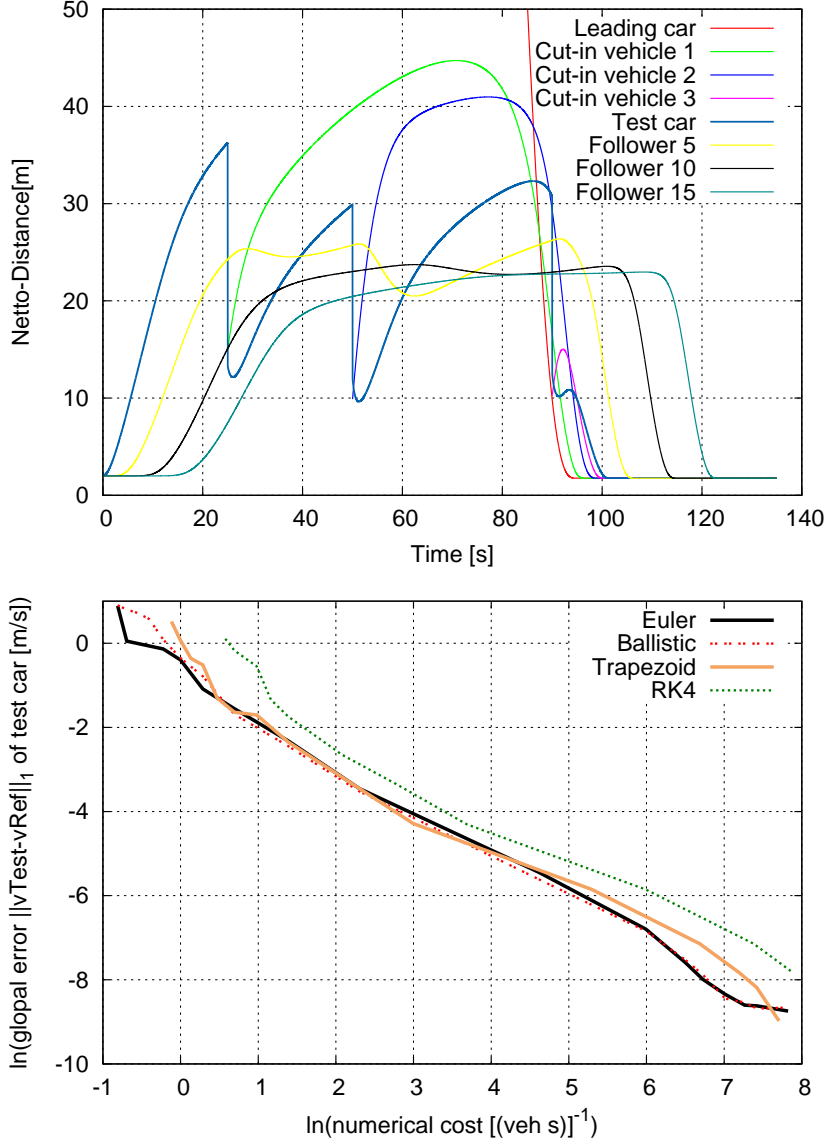


Fig. 9. Top: gap in front of the test vehicle. The three discontinuities represent three vehicles merging in front of this vehicle; bottom: convergence diagram for the test vehicle.

dictors of RK4 err to such an extent that the result is essentially that of the ballistic method.

4.5 Lane Changes

The most severe source of discontinuities are active and passive lane changes, i.e., the considered vehicle changes itself, or another changing vehicle “cuts in” in front of it. From the mathematical point of view, this means that not

only the accelerations of the leader are discontinuous but the gaps and leading speeds as well. Since the two latter quantities are exogenous variables of the model’s acceleration functions, the acceleration profile of the vehicle behind the lane-changing vehicle on the target lane is discontinuous as well reducing the consistency orders of all methods to $p = 1$.

This is, in fact, what we observe: Figure 9 displays a simulation where the test vehicle encounters three cut-ins in front of it. All four integration methods have the empirical consistency order $p = 1$. Remarkably and unexpectedly, the absolute value of the error for a given numerical cost is largest for RK4.

5 Discussion and Conclusions

In this work, we have systematically investigated the global discretization error of several explicit numerical integration schemes commonly used for simulating time-continuous car-following models. To enable an equitable comparison between simple and higher-order methods, we have determined the errors as a function of the numerical complexity, i.e., the normalized computation time for simulating one vehicle over one time unit: A method is better if, for the same numerical complexity, its global errors are lower.

Generally, when integrating ODEs or systems thereof, the fourth-order Runge-Kutta scheme (RK4) is the *de-facto* standard and other methods are rarely used. Why is this not the case for integrating car-following models where Euler’s method is most widespread? This contribution shows that, for typical traffic-related situations, the RK4 method is, in fact, not the best method since the smoothness conditions to reach its theoretical consistency order $p = 4$ are rarely given. To investigate the effect of violating these conditions, we simulated several scenarios and several models, from the ideal case to the most severe violations of smoothness:

- (1) All trajectories remain smooth (sufficiently often differentiable) over the complete simulation time (Sect. 4.1),
- (2) the acceleration profile of the trajectories is continuous but not smooth due to the model’s acceleration function (Sect. 4.3 or the external data (Sect. 4.4),
- (3) the acceleration profile is discontinuous due to stopped vehicles (Sect. 4.2) or by discontinuities in the model’s acceleration function which are reached by the system dynamics (Fig. 8),
- (4) the speed and gap profiles are discontinuous as a consequence of lane changes (Sect. 4.5).

We have found that RK4 and the trapezoidal scheme perform best if the trajec-

tories are smooth or have, at most, kinks in the acceleration. With our special treatment of stopping vehicles (Sec.2.4), this also carries over to stops with a discontinuous acceleration. In all other situations, however, the consistency order of *all* methods is restricted to one and the ballistic and trapezoidal schemes are equally performant as RK4. Moreover, when including lane changes, RK4 turned out to have the worst performance, even worse than simple Euler.

In summary, we recommend the ballistic and trapezoidal methods as efficient and robust schemes for integrating car-following models. Although of the same theoretical consistency order $p = 1$ as Euler’s method, the ballistic scheme turned out to be *consistently* better than Euler’s scheme with typically only about 30 % of the discretization errors compared to the latter method.

References

- Aw, A., Klar, A., Rascle, M., Materne, T., 2002. Derivation of continuum traffic flow models from microscopic follow-the-leader models. *SIAM Journal on Applied Mathematics* 63 (1), 259–278.
- Bando, M., Hasebe, K., Nakayama, A., Shibata, A., Sugiyama, Y., 1994. Structure stability of congestion in traffic dynamics. *Japan Journal of Industrial and Applied Mathematics* 11 (2), 203–223.
- Behrisch, M., Bieker, L., Erdmann, J., Krajzewicz, D., 2011. Sumo-simulation of urban mobility-an overview. In: *SIMUL 2011, The Third International Conference on Advances in System Simulation*. pp. 55–60.
- Casas, J., Ferrer, J. L., Garcia, D., Perarnau, J., Torday, A., 2010. Traffic simulation with aimsun. In: *Fundamentals of Traffic Simulation*. Springer, pp. 173–232.
- Gazis, D. C., Herman, R., Rothery, R. W., 1961. Nonlinear follow-the-leader models of traffic flow. *Operations Research* 9 (4), 545–567.
- Helbing, D., Tilch, B., 1998. Generalized force model of traffic dynamics. *Physical Review E* 58, 133–137.
- Helly, W., 1959. Simulation of bottlenecks in single lane traffic flow. In: *General Motors Research Laboratories (Ed.), Proceedings of the Symposium on the Theory of Traffic Flow*. Elsevier, New York, pp. 207–238.
- Jamison, S., McCartney, M., 2009. Discrete vs. continuous time implementation of a ring car following model in which overtaking is allowed. *Nonlinear Analysis: Real World Applications* 10 (1), 437–448.
- Jiang, R., Wu, Q., Zhu, Z., 2001. Full velocity difference model for a car-following theory. *Physical Review E* 64, 017101.
- Kaupuzs, J., Weber, H., Tolmacheva, J., Mahnke, R., 2004. Applications to traffic breakdown on highways. In: *Progress in Industrial Mathematics at ECMI 2002*. Springer, pp. 133–138.
- Kesting, A., Treiber, M., 2008. How reaction time, update time and adapta-

- tion time influence the stability of traffic flow. *Computer-Aided Civil and Infrastructure Engineering* 23, 125–137.
- Newell, G., 1961. Nonlinear effects in the dynamics of car following. *Operations Research* 9, 209.
- Quarteroni, A., Sacco, R., Saleri, F., 2007. *Numerical mathematics*. Vol. 37. Springer.
- Schakel, W. J., Knoop, V. L., van Arem, B., 2012. Integrated lane change model with relaxation and synchronization. *Transportation Research Record: Journal of the Transportation Research Board* 2316 (1), 47–57.
- Shamoto, D., Tomoeda, A., Nishi, R., Nishinari, K., Apr 2011. Car-following model with relative-velocity effect and its experimental verification. *Phys. Rev. E* 83, 046105.
- Treiber, M., Hennecke, A., Helbing, D., 2000. Congested traffic states in empirical observations and microscopic simulations. *Physical Review E* 62, 1805–1824.
- Treiber, M., Kesting, A., 2013. *Traffic Flow Dynamics: Data, Models and Simulation*. Springer, Berlin.